Journal of the European Ceramic Society 19 (1999) 389–397

PII: S0955-2219(98)00199-X
0955-2219/99/$—see front matter

Characterization and Sintering of Gels in the System $MgO–Al_2O_3–SiO_2$

M.-A. Einarsrud,* S. Pedersen, E. Larsen and T. Grande

Department of Inorganic Chemistry, Norwegian University of Science and Technology, 7034 Trondheim, Norway

(Received 16 January 1998; revised version received 27 July 1998; accepted 6 August 1998)

Abstract

Cordierite aerogels, made by supercritical drying, and xerogels, formed by ambient pressure drying, have been prepared by combining two different recipes. The chemical composition of the gels varied from stoichiometric cordierite $2MgO·Al_2O_3·5SiO_2$ to $0·5MgO·1·4Al_2O_3·5SiO_2$ due to different procedures for washing of the gels. The crystallization of nearly stoichiometric cordierite gels was shown to be relatively complex involving the formation of several metastable phases such as μ-cordierite ($Mg_2Al_4Si_5O_{18}$), spinel ($Al_6Si_2O_{13}$) and sapphirine ($Mg_4Al_8Si_2O_{20}$) before the equilibrium phase composition was obtained at around 1350°C. On the other hand, during crystallization of gels with stoichiometry close to $0·5MgO·1·4Al_2O_3·5SiO_2$ the equilibrium phases mullite, cristobalite and α-cordierite were the major phases formed during heat treatment. A lower densification rate was observed for aerogels compared to xerogels due to a larger pore size. A lower crystallization temperature in aerogels probably due to heterogeneous nucleation reduced the densification. For gels with a composition near $0·5MgO·1·4Al_2O_3·5SiO_2$ nucleation and densification occur simultaneously and large differences in the densification behavior was observed. © *1999 Elsevier Science Limited. All rights reserved*

Keywords: sol–gel processes, silicate, cordierite, sintering, precursors.

1 Introduction

Cordierite based ceramics are attractive materials for several applications due to their electrical and thermal properties. Catalytic exhaust supports are based on cordierite and due to the low dielectric constant and low thermal expansion cordierite is interesting as substrate material for integrated circuits in electronics.[1–4] Cordierite is also an interesting insulator and refractory material due to its low thermal expansion and hence relatively large thermal shock resistances.[5]

One of the most difficult problems with the preparation of cordierite ceramics is the narrow temperature interval for sintering which is located just below the incongruent melting point of pure cordierite.[3] This narrow temperature interval demands reasonably well controlled temperature conditions during densification. Preparation from amorphous precursors or glasses has encountered problems due to the formation of the metastable modification μ-cordierite[6–11] and/or spinel.[9–11]

The interest in preparation of ceramic components by the sol–gel method has been increasing the last couple of decades. This method has the advantage of an excellent control of chemical composition and the possibility of reducing the temperature of ceramic processing. Thin films or other desired material designs can also be achieved. During the last years we have studied preparation and properties of monolithic silica xerogels and aerogels.[12–14] For the preparation of xerogels and aerogels washing of the gels prior to drying is most often necessary to exchange solvent or to remove water from the pore liquid.[13–16] Washing of cordierite gels has also been reported in the literature.[15] We have observed that during washing of wet cordierite gels, especially Mg and Al ions are extracted from the gel which modify the overall composition of the gel.[17] The loss of Mg and Al from the gels during washing was found to depend on the structure of the gel as well as the homogeneity of the wet gels.[17]

In this work we have studied the formation of oxide ceramics in the $MgO–Al_2O_3–SiO_2$ system by heat treatment of amorphous precursors formed by sol–gel processing. The gels were prepared using two

*To whom correspondence should be addressed. E-mail: mariann.einarsrud@chembio.ntnu.no

alkoxides, tetraethoxysilane (TEOS) and aluminum *sec*-butoxide (ASB), and a magnesium salt, using similar procedures as reported previously.[9,11,15,17,18] Gels with different chemical composition, gel structure and homogeneity have been obtained by a combination of two different gel recipes and by modifying the *washing* procedure of the gels prior to drying. The densification and crystallization of the gels are discussed in relation to chemical composition of the gels and the gel structure.

2 Experimental Procedure

Rod shaped monolithic wet gels (diameter about 8·5 mm) of cordierite stoichiometry were prepared from tetraethoxysilane (TEOS), aluminum *sec*-butoxide (ASB) complexed with acetyl acetonate (acac) to reduce the hydrolysis rate, and either magnesium acetate (gels of type **A**) or magnesium nitrate (gels of type **N**). The procedures are modified versions of the recipes reported by Selvaraj *et al.*[10] and Heinrich *et al.*,[15] respectively, and is schematically illustrated in Fig. 1. After the gel formation, the samples were washed by exchanging the surrounding liquid of the gels four times within 24 h. Four different washing procedures using ethanol, acetone, *n*-heptane and/or liquid CO_2 were applied. The washing was performed at 50°C using *n*-heptane and ethanol, 15–20°C for liquid CO_2 and 20–25°C for acetone. Finally, the gels were dried either at the *supercritical* conditions of CO_2, giving *aerogels*, or at *ambient* pressure at a temperature close to the boiling point of solvent, giving *xerogels*.[17] For the aerogels, the last solvent was liquid CO_2.

The gels were heat treated in air, at 500°C for type **A** gels and at 600°C for type **N** gels, for 1 week to remove organic residue from the alkoxides prior to further analysis. A higher temperature was chosen for the type **N** gels due to a smaller pore size. Thereafter the gels were sintered in air at various temperature between 800 and 1400°C for 6 h using a heating rate of $30\,K\,h^{-1}$ and a cooling rate of $250\,K\,h^{-1}$. The uncertainty of the sintering temperatures is estimated to be ± 5°C.

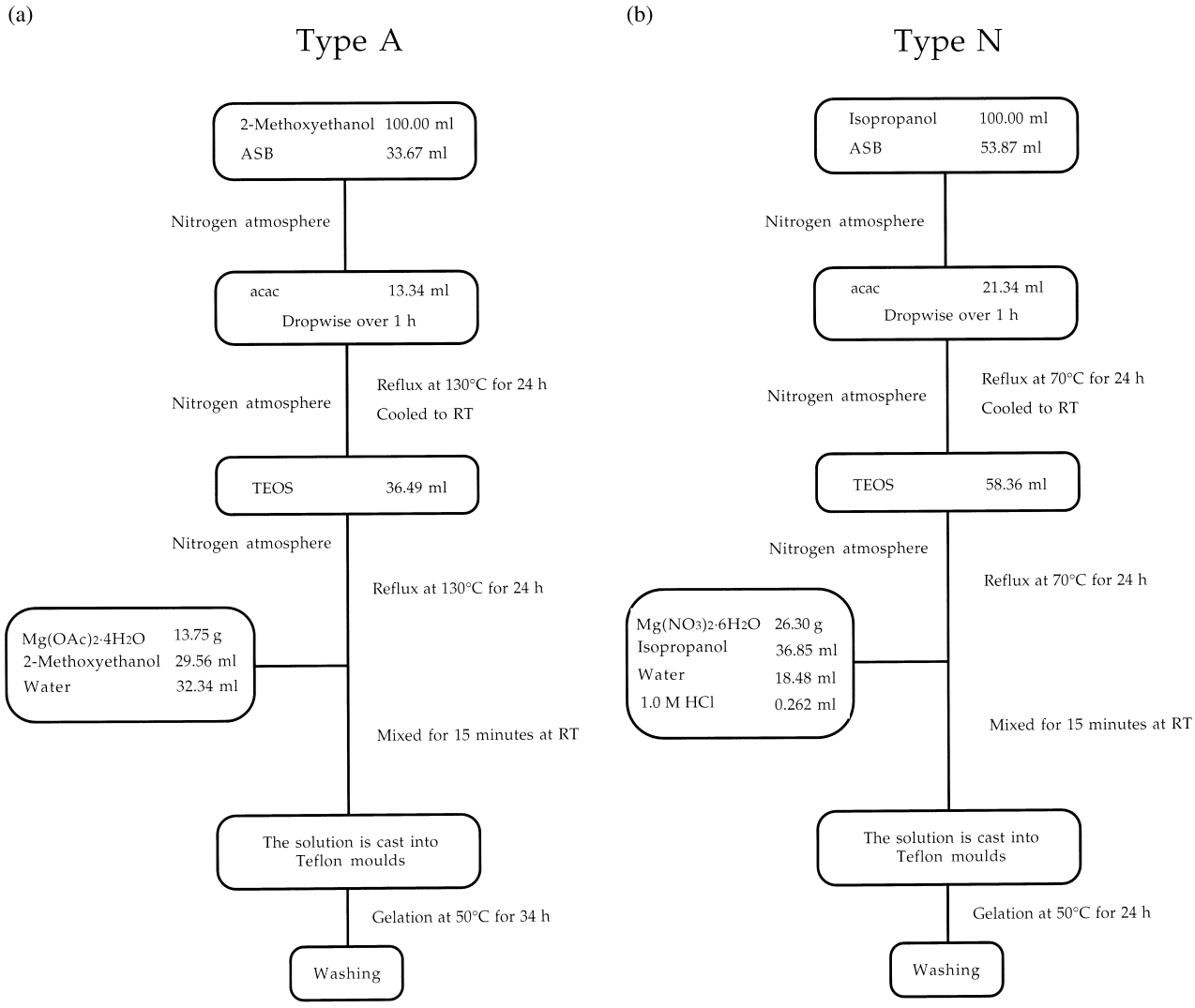

Fig. 1. Schematic presentation of the synthesis routes for gels of (a) type **A** and (b) type **N**.

Differential thermal analysis (DTA) was performed using a laboratory-built equipment. A Kanthal A wound tube furnace was used and the samples were heated using a constant power input. The average heating rate above 800°C was approximately $8\,K\,min^{-1}$. Prior to the measurement, the gels were crushed and mixed with a few droplets of ethanol and compressed into a platinum crucible. About 3 g of gel was used for the measurement, and corundum (Al_2O_3) was used as reference material.

Powder XRD (Philips PW 1730/10) using CuK_α radiation (scan rate $0{\cdot}02°/s^{-1}$ in the region from 7 to 70° 2θ) was used for qualitative and quantitative identification of crystalline phases. Unit cell parameters of μ-cordierite found in heat treated gels of type **A** were calculated by using the program MICRO CellRef (Materials Data Inc.) and the reflections 110, 102, 200, 201, 112 and 211.

The surface area of the gels was measured by N_2 adsorption (Micromeritics, ASAP 2000) and calculated using the five point BET theory. The densities of the gels were calculated from the mass and volume of the samples. The hydraulic radii, r_h, were calculated from the formula, $r_h = 2V_p/SA$, where SA is the measured surface area and V_p the pore volume calculated from the aero- or xerogel density and a skeletal density of $2{\cdot}5\,g\,cm^{-3}$, which was the maximum density obtained after densification.

3 Results

The composition of the present gels given in Table 1 were measured by chemical analysis and X-ray diffraction.[17] Due to different washing procedures the composition of the gels varied ranging from nearly pure cordierite $2MgO{\cdot}2Al_2O_3{\cdot}5SiO_2$ to about $0{\cdot}5MgO{\cdot}1{\cdot}4Al_2O_3{\cdot}5SiO_2$. All gels were monolithic after drying except for the non-washed gels of type **N** which powdered during the drying procedure and the non-washed supercritically dried gels of type **A** which were brittle and disintegrated.

Table 1. Composition of gels after washing and drying[17]

Sample	*Mg*	*Al*	*Si*	*Al/Si*
AX	1·92	3·84	5	2·00
AXE	1·49	3·12	5	2·09
AXA	1·86	3·72	5	2·00
AXEH	1·49	3·10	5	2·08
AA	1·92	3·84	5	2·00
AAE	1·45	3·03	5	2·09
AAA	1·86	3·72	5	2·00
NXE	0·69	2·74	5	3·97
NXA	0·75	2·80	5	3·73
NXEH	0·65	2·75	5	4·23
NAE	0·65	2·78	5	4·28
NAA	0·67	2·76	5	4·12
NAEA	0·61	2·70	5	4·43
Cordierite	2	4	5	2·00

Basis is taken in the cordierite composition Mg:Al:Si = 2:4:5. The errors of the calculated compositions are estimated to +10 and −5%.

The density, surface area and hydraulic radius of the gels after heat treatment at 500–600°C are given in Table 2 as well as the surface area and hydraulic radius after sintering at 800°C. The density of the gels after isothermal sintering to temperatures in the interval 800–1400°C is shown in Fig. 2. The final density of the dried gels is determined by the capillary tension developed during the drying (dependent on pore size and surface tension of the pore liquid) and the bulk modulus of the drained network.[19] Assuming that all the gels of the same type (either **A** or **N**) have the same modulus and pore dimensions, the density of the gels is determined by the surface tension of the solvent removed during drying. Hence the xerogels dried from *n*-heptane [γ_{LV}, *n*-heptane (90°C) = $13{\cdot}4\,dyne/cm^{-1}$; Ref. 20] show a much lower density than the xerogels dried from either ethanol [γ_{LV}, ethanol (70°C) = $18{\cdot}2\,dyne\,cm^{-1}$; Ref. 21] or acetone [$\gamma_{LV}$, acetone (50°C) = $19{\cdot}9\,dyne\,cm^{-1}$; Refs 20 and 21]. However, the supercritical dried gels have the lowest density. The pore size represented by the hydraulic radius is following the density for each type of gel. However, r_h is significantly higher for the type **A** gels when gels dried from the same type of solvent are compared. Prior to sintering there is no significant difference in surface area for aerogels and xerogels as is expected from the literature,[22] however; the type **N** gels have a slightly higher surface area.

DTA heating curves for the gels of type **A** are shown in Fig. 3(a). Two exothermic peaks are observed for the non-washed (AX, AA) and acetone-washed gels (AXA), while only one was observed for the ethanol-washed gels (AXE, AXEH, AAE) and the acetone-washed aerogel (AAA). The exothermic features are interpreted as crystallization of μ- and α-cordierite based on XRD analysis of the samples after the DTA. Crystallization temperatures (T_μ, T_α) and phase composition of the type **A** gels are given in Table 3.

The DTA heating curves for the gels of type **N** are shown in Fig. 3(b). Only a single sharp exothermic peak is evident for all the type **N** gels except for the non-washed (NX) gel for which two exothermic peaks appeared. Mullite was the only crystalline phase found in the washed gels which corresponds well with only a single crystallization peak. Crystallization temperatures (T_μ, T_α, T_M) and the phase composition of the type **N** gels are given in Table 4.

The phases observed in the heat treated gels of type **A** are summarized in Table 5. Representative

Table 2. Density, surface area and calculated hydraulic radius after heat treatment to 500–600°C for gels of type **N** and **A** as well as the surface area and calculated hydraulic radius after sintering to 800°C

Sample code	*Density ±3% (g cm^{-3})*	*Surface area (500/600°C) ±5% (m^2 g^{-1})*	*Surface area (800°C) ±5% (m^2 g^{-1})*	*Hydraulic radius (500/600°C) ±6% (Å)*	*Hydraulic radius (800°C) ±6% (Å)*
AX	1·04	434	95	26	—
AXE	1·20	495	128	18	23
AXA	1·19	428	—	20	—
AXEH	0·76	534	—	34	—
AA	0·32	332	—	164	—
AAE	0·22	526	239	159	187
AAA	0·22	468	—	182	—
NXE	1·29	562	226	13	19
NXA	1·32	525	223	14	19
NXEH	0·91	611	311	23	30
NAE	0·26	—	343	—	143
NAA	0·26	591	322	117	153
NAEA	0·27	591	329	113	149

The samples are labelled according to the following procedure: the first letter is the gel type (**A** or **N**), the second reflects the drying procedure (xerogel = X, or aerogel = A) and last the solvent(s) used for washing (ethanol = E, acetone = A, or n-heptane = H)

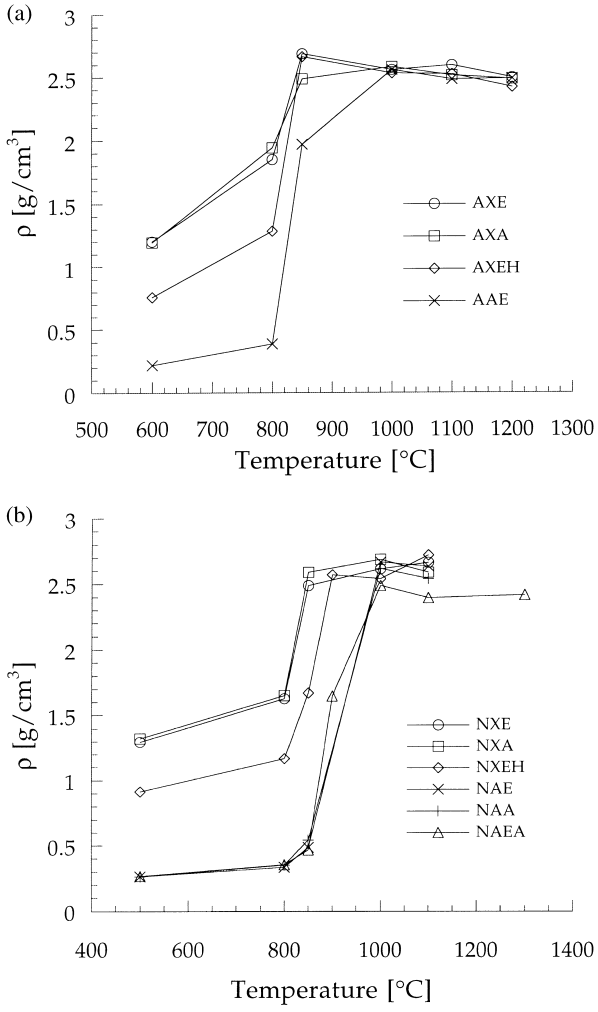

Fig. 2. Density of gels of (a) type **A** and (b) type N as function of heat treatment temperature. The gels were sintered for 6 h at maximum temperature. Uncertainty in density is ±3%.

X-ray diffractograms of three typical samples are shown in Fig. 4(a)–(c). At 850°C, the gels are still amorphous and the diffraction patterns show a broad halo at 3·57 Å with a ridge around 6·4 Å. After sintering at 1000°C, μ-cordierite was the major phase in addition to the remaining amorphous matrix. In the non-washed xerogel (AX), μ-cordierite gradually disappeared and increasing amounts of α-cordierite and spinel were observed with increasing heat treatment temperature up to 1200°C [Fig. 4(a)]. After sintering at 1350°C the sample appeared as nearly phase pure α-cordierite with possible traces of cristobalite. In the acetone-washed gels (AXA, AAA) [Fig. 4(b)], μ-cordierite transformed to α-cordierite upon further heat treatment. For the ethanol-washed gels (AXE, AXEH, AAE) the development of the phase compositions were more complicated as shown in Fig. 4(c). Already at 1000°C, μ-cordierite, cristobalite and spinel had been formed. At 1100°C some of the μ-cordierite had been transformed to α-cordierite and the amount of cristobalite and spinel had increased. At 1200°C, α-cordierite and cristobalite were observed together with sapphirine and possible traces of mullite. At 1350°C no amorphous phase remained and the three phases α-cordierite, cristobalite and mullite coexisted.

Unit cell parameters of μ-cordierite in gels of type **A** after heat treatment at 1000°C are reported in Table 6. The unit cell parameter a was significantly larger for the non-washed gels. Among the washed gels, a was higher for the acetone-washed gels compared to the ethanol-washed gels.

All the washed gels of type **N** followed the same crystallization behavior. XRD patterns for a typical sample are shown in Fig. 4(d). At 850°C the gels were still amorphous showing a broad halo around 3·87 Å and a ridge at about 6·9 Å. After heat treatment at 900°C, mullite had crystallized and up to 1100°C there is no significant differences in the diffractograms. After heat treatment at 1300°C the predominant phase was cristobalite

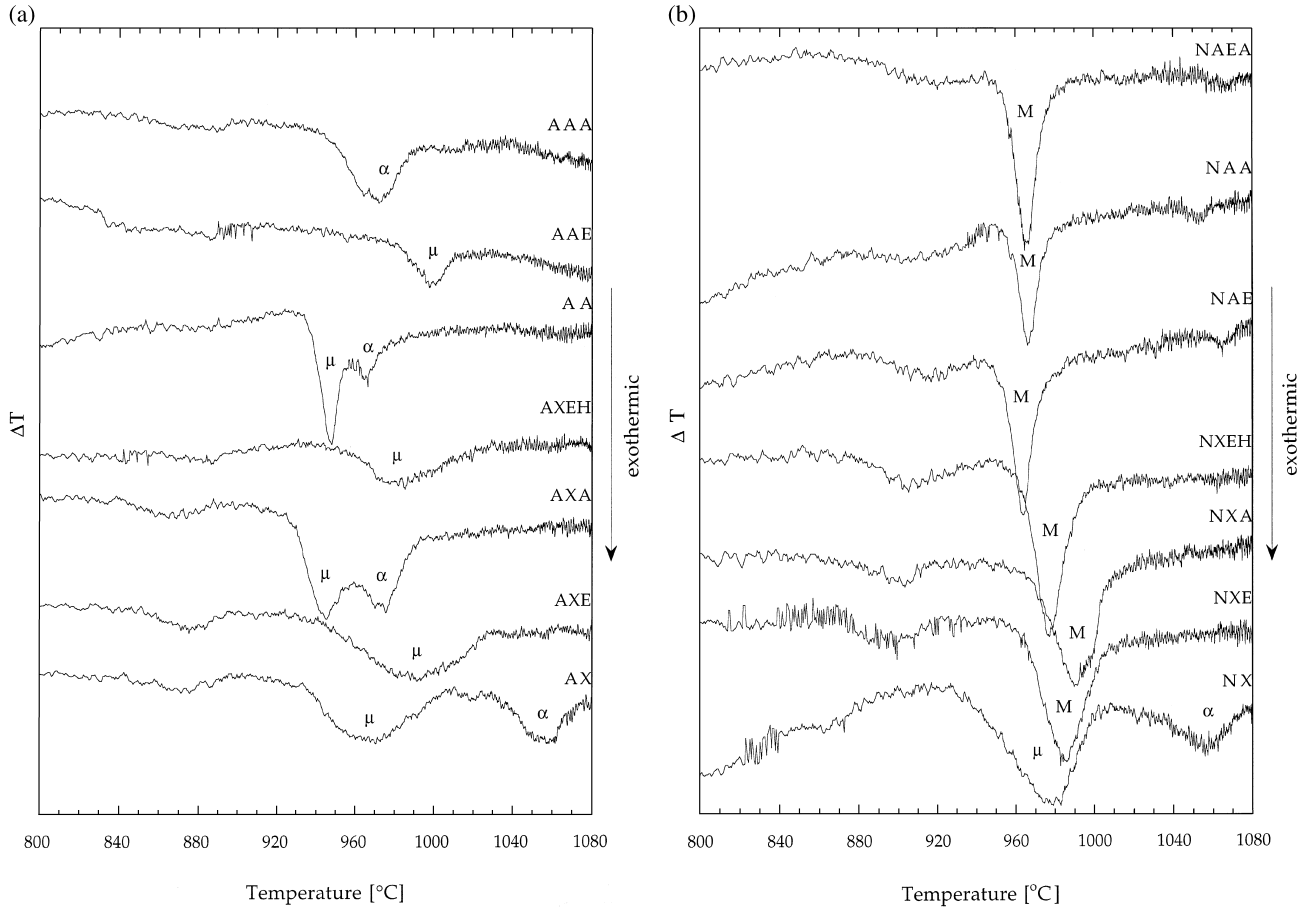

Fig. 3. DTA data of gels of (a) type **A** and (b) type **N**. Crystallization peaks are marked with the respective phases: M, mullite; μ, μ-cordierite; and α, α-cordierite.

together with small amounts of α-cordierite. Traces of sapphirine were also possible present. The amount of cristobalite has decreased to some degree after heat treatment at 1400°C compared to 1300°C.

4 Discussion

Due to the high crystallization temperature and the low initial density of the gels, DTA was performed by using a cell constructed in our laboratory. The crushing and compression of the gel prior to the measurement could possibly induce nucleation centers in the sample. Monolithic gels might therefore crystallize following somewhat different routes than observed during the DTA-measurements.

A weak endothermic shift in the DTA baseline prior to the crystallization were evident in the majority of the DTA-curves shown in Fig. 3. This particular feature has been interpreted as a signature of a gel to viscous liquid transition or glass transition. Compared to glasses prepared by cooling the liquid through the glass transition, a gel with the corresponding chemical composition would most likely possess a higher free energy.[23] An exothermic relaxation of the gel is therefore

Table 3. Crystallization temperatures of μ- (T_μ) and α-cordierite (T_α) obtained by DTA for type **A** gels. Crystalline phases observed by XRD after DTA to 1080°C are included

Sample	T_μ *(°C)* ±3°C	T_α *(°C)* ±3°C	*Phases after DTA*	
			Major	*Minor*
AAA	—	944	α	—
AAE	979	—	μ	α
AA	934	947	α	—
AXEH	957	—	μ	—
AXA	927	962	α	—
AXE	938	—	μ	—
AX	931	1035	α	—

Table 4. Crystallization temperatures of μ (T_μ), α-cordierite (T_α) and mullite (T_M) obtained by DTA for type **N** gels. Crystalline phases observed by XRD after DTA to 1080°C are included

Sample	T_M *(°C)* ±3°C	T_μ *(°C)* ±3°C	T_α *(°C)* ±3°C	*Phases after DTA*	
				Major	*Minor*
NAEA	953	—	—	M	α
NAA	953	—	—	M	—
NAE	951	—	—	M	α
NXEH	961	—	—	M	μ
NXA	966	—	—	M	μ
NXE	963	—	—	M	μ
NX	—	928	1030	α	—

Table 5. Crystalline phases observed in gels of type **A** heat treated for 6 h at various temperatures

Sample	*1000°C*	*1100°C*	*1200°C*	*1350°C*
AX	μ, am, (α)	μ, α, am, (sp)	μ, α, am, (sp)	α, c
AXE	μ, am, (c, sp)	αc, μ, am, (sp)	α, c, sa, am	α, (c, M)
AXA	μ, am	α, μ, am	α, am	α, (c)
AXEH	μ, am	α, c, μ, am, (sp)	α, c, am, sa	α, (c, M)
AA	μ, am	—	—	α, c
AAE	μ, am	μ, c, sp, am	c, sa, α, am	α, c, (M)
AAA	μ, am	μ, α, am	α, am	α, (c)

The following abbreviations are used for the phases present: am: amorphous, α: α-cordierite, c: cristobalite, μ: μ-cordierite, M: mullite, sa: sapphirine; sp: spinel. Minor phases are given in parentheses.

most likely to occur near the glass transition. However, when passing through the glass transition region one would also expect to observe, superimposed on the exothermic relaxation, an endothermic shift due to the effect of going from a glass to a supercooled liquid. Ideally this would also be the case in our DTA-experiments. However, for all our experiments, in addition to a relatively high signal to noise ratio, a significant drift in the baseline occurred. It was therefore difficult to determine the glass transition temperature (T_g). The observed glass transition regions were observed above T_g for cordierite, which is reported at 822°C by Mazurin *et al.*[24] With decreasing Mg and Al content, T_g have been reported to increase.[24] We would therefore expect the glass transition to occur at a higher temperature for the gels of type **N** compared to the gels of type **A** as confirmed by the DTA curves.

For gels of type **A** with two exothermic crystallization peaks [Fig. 3(a)], the second exothermic peak was interpreted as formation of α-cordierite. The interpretation is based on the DTA/XRD analysis and the XRD analysis of the heat treated monolithic samples. α-cordierite was observed as the major phase in all samples exhibiting two crystallization peaks, while primarily only μ-cordierite was observed for samples with only a single crystallization event. However, the acetone-washed aerogel (AAA) crystallizes directly to α-cordierite. The formation of α-cordierite can either be in the residual amorphous phase or precipitate out from the μ-cordierite solid solution. Reported crystallization of cordierite powders and gels corresponds with our findings although reported crystallization of α-cordierite is somewhat higher and varies from 975 to 985°C and the formation of α-cordierite appears between 1000 to 1080°C.[8,10,11,25] It is also interesting to note from Fig. 3(a) that the crystallization of the non-washed aerogel (AA) to μ- and α-cordierite occur at significantly lower temperatures compared to the non-washed xerogel (AX). A similar behavior is also observed for the type **N** gels. From this observation we can assume that heterogeneous nucleation is important for the crystallization behavior of the gels and this will be further discussed in the following.

The formation of α-cordierite in the acetone-washed gels of type **A** occurred at temperatures below 1000°C during the DTA-measurements. However, formation of α-cordierite did not occur during sintering of monolithic gels of type **A** at 1000°C. The crushing and compression of the gels performed prior to the DTA did therefore enhance the formation of α-cordierite. The most probable explanation is that surface nucleation of α-cordierite has occurred in the powdered gels.

The crystallization of the type **N** gels did mainly involve formation of the stable crystalline phases mullite, cristobalite and α-cordierite except for the traces of sapphirine observed at 1300°C. Crystallization of mullite is observed already at 900°C [Fig. 4(d)] which is only some tens of degrees above the glass transition temperature and in fact below the thermodynamic stability region in the binary system Al_2O_3–SiO_2.[26] From Fig. 3(b) it is observed that the crystallization temperature for mullite is lower for aerogels than for xerogels and it is lower for the xerogels dried from *n*-heptane than the other xerogels. Formation of α-cordierite and cristobalite does not occur before heat treatment at 1300°C. The high crystallization temperature of these two phases is probably caused by the high content of SiO_2 and hence increased viscosity in the remaining liquid after crystallization of mullite.

The crystallization of some of the gels of type **A** is a relatively complex chemical process involving the formation of several metastable phases such as μ-cordierite, spinel and sapphirine. The first phase to occur in all the **A**-type gels is μ-cordierite reflecting that the local gel structure is probably close to the local order in crystalline μ-cordierite. μ-cordierite forms solid solutions with quartz over a wide composition range from pure SiO_2 to $MgAl_2O_4$.[27] In some of the gels (AXA, AAA), the phase evolution follows a simple transition to the dominant equilibrium phase α-cordierite and possible traces of cristobalite. In these gels the last traces of μ-cordierite have disappeared during heat treatment at 1200°C. The coexistence of α- and

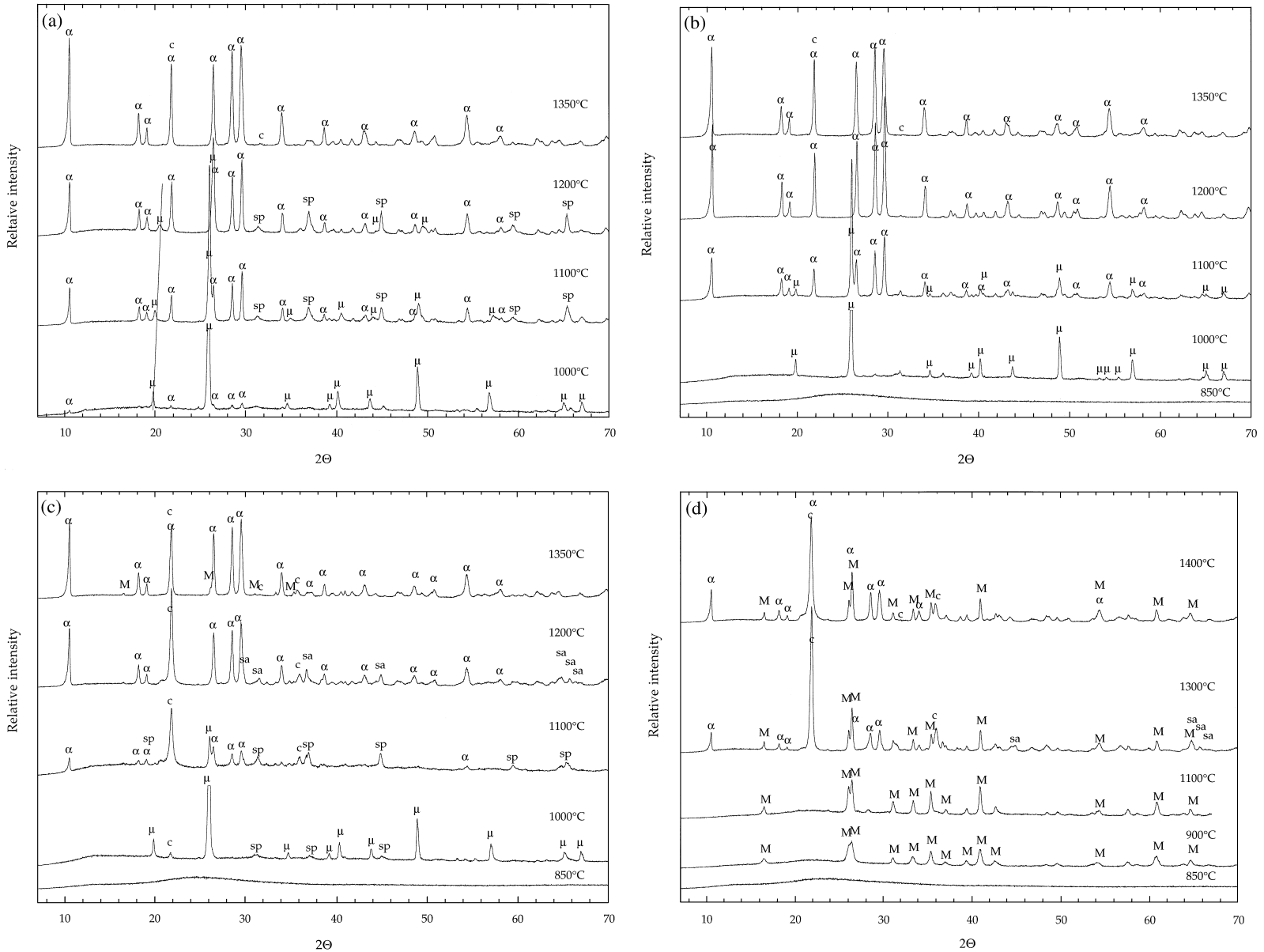

Fig. 4. Development of X-ray diffractograms with increasing heat treatment temperature for (a) AX, (b) AXA, (c) AXE, and (d) NXEH gels. The observed phases are marked as follows: α, α-cordierite; μ, μ-cordierite; c, cristobalite; M; mullite; sa, sapphirine; and sp, spinel. (The intensity of the diffraction peak for α-cordierite at 4·064 Å is higher than expected for pure α-cordierite phase. This peak can overlap with the 100% peak for cristobalite at 4·0397 Å). CuK_α radiation with $\lambda = 1{\cdot}54179$ Å was used.

Table 6. Cell parameters, a and c, of μ-cordierite crystallized at 1000°C from gels of type **A**

Sample	a *(Å)* ± 0·003 *Å*	c *(Å)* ± 0·003 *Å*
AX	5·190	5·343
AXE	5·169	5·363
AXA	5·182	5·352
AXEH	5·176	5·364
AA	5·194	5·347
AAE	5·176	5·357
AAA	5·183	5·345

μ-cordierite over a wide temperature range indicates that α-cordierite is formed by a nucleation and growth mechanism and probably not through a solid state phase transition. For some of the gels even spinel and sapphirine have crystallized. These phases are not at all equilibrium phases according to the overall chemical composition. However, according to the phase diagram,[28] metastable extensions of the primary crystallization surfaces of these two phases will cross at temperatures well above the temperature where they were observed to be formed. The phases are therefore thermodynamically stable relative to the remaining supercooled liquid. Equilibrium phase composition is achieved after heat treatment at 1350°C.

Schreyer *et al.*[27] reports the cell parameters for μ-cordierite crystallized from glasses with initially variant composition on the tieline SiO_2–$MgAl_2O_4$. Increasing the amount of magnesium and aluminum ions within the quartz structure would cause a small shrinkage of the c-axis of the crystals and a larger expansion in the a-direction. The variation in the a parameter given in Table 6 is in fairly good agreement with the change in composition reported in Table 1. Amista *et al.*[29] observed an increase in the crystallization peak temperature for the μ-cordierite phase with increasing silica content for melt quenched glasses. Comparing similar gels with different composition we see the same tendency.

The densification of the gels were observed to occur between 800 and almost 1000°C as can be seen from Fig. 2. The densification rate for viscous flow is dependent on the composition of the gel which determines the viscosity and the pore size of the gel.[23] By comparing the data for the type **A** gels in Fig. 3(a), the xerogels show a similar densification behavior while the aerogel densities at a slightly higher temperature. From Fig. 2(a) it can be seen that there is no connection between the gel composition (Table 1) and the densification rate. Hence, the increase in sintering temperature for the aerogel must be due to the higher pore size of this gel (Table 2) giving a lower densification rate.[23] It should also be mentioned that the type **A** gels sinters to theoretical density prior to crystallization which is also previously reported in literature.[6,9] However, as shown in Fig. 3(a) the aerogel (AA) crystallized at a lower temperature than the xerogel (AX). This crystallization behavior can be explained by the reduced densification rate of the aerogels due to a larger pore size, and hence they have a larger surface area at a given temperature (compare $239\,m^2\,g^{-1}$ for aerogels and $128\,m^2\,g^{-1}$ for xerogels at 800°C). The larger surface area enhances surface nucleation.

The silica rich type **N** gels [Fig. 2(b)] with only minor differences in composition (Table 1) show large differences in densification behavior. This observed difference is too large to be explained by the different pore sizes of xerogels and aerogels, i.e. compare type **A** gels. The NXE and NXA gels show a similar densification behavior as the type **A** gels and sinter to theoretical density at about 850°C which is below the crystallization temperature of mullite. However, for the aerogels and possibly for the xerogels dried from *n*-heptane, crystallization of mullite occurs before a complete densification has occurred. The lower crystallization temperature of the aerogels and xerogels dried from *n*-heptane compared to xerogels dried from ethanol or acetone is confirmed by DTA [Fig. 3(b)] and Table 4. We believe this lower crystallization temperature is caused by the larger surface area of the aerogels at a given temperature due to a lower densification rate as explained in the preceding section. Table 2 gives a surface area of the aerogels of $320–340\,m^2\,g^{-1}$ while the xerogels have a surface area of about $220\,m^2\,g^{-1}$. Hence the degree of surface nucleation is higher for the aerogels. When mullite is crystallizing, the supercooled liquid becomes enriched in SiO_2 and hence it obtains a higher viscosity. With increasing viscosity the sintering is suppressed and a significant increase in sintering temperature is observed.

5 Conclusion

Aerogels and xerogels in the system MgO–Al_2O_3–SiO_2 with stoichiometry ranging from cordierite, $2MgO{\cdot}Al_2O_3{\cdot}5SiO_2$, to $0{\cdot}5MgO{\cdot}1{\cdot}4Al_2O_3{\cdot}5SiO_2$ have been prepared using two different recipes and different washing procedures. Gels close to the cordierite stoichiometry show a relatively complex crystallization behavior involving the formation of several metastable phases such as μ-cordierite, spinel and sapphirine before the equilibrium phase composition occurs at 1350°C. On the other hand, during crystallization of gels with stoichiometry close to $0{\cdot}5MgO{\cdot}1{\cdot}4Al_2O_3{\cdot}5SiO_2$ mostly the equilibrium phases mullite, cristobalite and α-cordierite were observed.

The larger pore size of the aerogels compared to xerogels decreases the densification rate and hence the aerogels have a higher surface area at a given temperature. This larger surface area is shown to decrease the crystallization temperature probably due to heterogeneous nucleation. For gels with a stoichiometry close to $0{\cdot}5MgO{\cdot}1{\cdot}4Al_2O_3{\cdot}5SiO_2$, the nucleation and densification is taking place in the same temperature interval and large differences in the densification behavior was observed.

Acknowledgement

Financial support from Borgestads Legat is acknowledged.

References

1. Bridge, D. R., Holland, D. and McMillan, P. W., Development of the alpha-cordierite phase in glass ceramics for use in electronic devices. *Glass Techn*., 1985, **26**, 286–292.
2. Barry, T. I., Lay, L. A. and Morrell, R., Refractory glass-ceramics. *Proc. Brit. Ceram. Soc*., 1973, **22**, 27–37.
3. Morrell, R., The mineralogy and properties of sintered cordierite glass-ceramics. *Proc. Brit. Ceram. Soc*., 1979, **28**, 52–71.
4. Milberg, M. E. and Blair, H. D., Thermal expansion of cordierite. *J. Am. Ceram. Soc*., 1977, **60**, 372–373.
5. Von Gugel, E., Indialith (Cordierit) als Basis temperaturwechselbeständiger feuerfester Baustoffe. *Ber. Dtsch. Keram. Ges*., 1967, **44**, 547–553.
6. Vesteghem, H., Di Giampaolo, A. R. and Dauger, A., Low temperature synthesis and sintering of sol–gel derived cordierite. *Science of Ceramics*, 1988, **14**, 321–326.
7. Suzuki, H., Ota, K. and Saito, H., Preparation of cordierite ceramics from metal alkoxides (Part 1). *Yogyo-Kyokai–Shi*, 1987, **95**, 163–169.
8. Zelinski, B. J. J., Fabes, B. D. and Uhlmann, D. R., Crystallization behavior of sol–gel derived glasses. *J. Non-Cryst. Solids*, 1986, **82**, 307–313.
9. Bernier, J. C., Rehspringer, J. L., Vilminot, S. and Poix, P., Synthesis and sintering comparison of cordierite powders. *Mat. Res. Symp. Proc*., 1986, **73**, 129–134.
10. Selvaraj, U., Komarneni, S. and Roy, R., Synthesis of glass-like cordierite from metal alkoxides and characterization by ^{27}Al and ^{29}Si MASNMR. *J. Am. Ceram. Soc*., 1990, **73**, 3663–3669.
11. Bonhomme-Coury, L., Babonneau, F. and Livage, J., Comparative study of various sol–gel preparations of cordierite using ^{27}Al and ^{29}Si liquid-and solid-state NMR spectroscopy. *Chem. Mater*., 1993, **5**, 323–330.
12. Hæreid, S., Dahle, M., Lima, S. and Einarsrud, M.-A., Preparation and properties of monolithic silica xerogels from TEOS-based alcogels aged in silarie solutions. *J. Non-Cryst. Solids*, 1995, **186**, 96–103.
13. Hæreid, S., Nilsen, E. and Einarsrud, M.-A., Subcritical drying of silica gels. *J. Porous Matr*., 1996, **2**, 315–324.
14. Scherer, G. W., Hæreid, S., Nilsen, E. and Einarsrud, M.-A., Shrinkage of silica gels aged in TEOS. *J. Non-Cryst. Solids*, 1996, **202**, 42–52.
15. Heinrich, T., Tappert, W., Lenhard, W. and Fricke, J., Synthesis and properties of mullite and cordierite aerogels. *J. Sol–Gel Sci. Tech*., 1994, **2**, 921–924.
16. Deshpande, R., Smith, D. M, and Brinker, C. J., Patent WO 94 25149.
17. Einarsrud, M.-A., Kirkedelen, M. B., Samseth, J., Mortensen, K., Grande, T. and Pedersen, S., Washing of multicomponent gels prior to drying. *J. Non-Cryst. Solids*, 1996, **215**, 169–175.
18. Babonneau, F., Coury, L. and Livage, J., Aluminum *sec*-butoxide modified with ethylacetoacetate: an attractive precursor for the sol–gel synthesis of ceramics. *J. Non-Cryst. Solids*, 1990, **121**, 153–157.
19. Scherer, G. W., Smith, D. M. and Stein, D., Deformation of aerogels during characterization. *J. Non-Cryst. Solids*, 1995, **188**, 309–315.
20. ES Software, *TAPP Thermochemical and Physical Properties*. 2234 Wade Court, Hamilton, OH 45013.
21. Dean, J. A. (ed.), *Lange's Handbook of Chemistry*, McGraw–Hill, New York, 1973, pp. 10-269-270.
22. Smith, D. M., Scherer, G. W. and Anderson, J. M., Shrinkage during drying of silica gels. *J. Non-Cryst. Solids*, 1995, **188**, 191–206.
23. Brinker, C. J. and Scherer, G. W., *Sol–Gel Science*. Academic Press, San Diego, CA, 1990.
24. Mazurin, O. V., Streltsina, M. V., and Shaiko-Shaikovskaya, T. P., *Handbook of Glass Data*. Part C, 758. Elsevier, Amsterdam, 1987, pp. 758.
25. Vesteghem, H., Di Giampaolo, A. R. and Dauger, A., Low-temperature cordierite glass from autoclave-prepared gel. *J. Mater. Sci. Lett*, 1987, **6**, 1187–1189.
26. Pask, J. A., Stable and metastable phase equilibria and reactions in the SiO_2-αAl_2O_3 system. *Ceram. Int*., 1983, **9**, 107–133.
27. Schreyer, W. and Schairer, J. F., Metastable solid solution with quartz-type structures on the joint $SiO_2–MgAl_2O_4$. *Zeitschrift für Krist*., 1961, **116**, 60–82.
28. Levin, M. E., Robbins, C. R. and McMurdie, H. F., *Phase Diagrams for Ceramists*. The American Ceramic Society, Columbus, OH, 1964.
29. Amista, P., Cesari, M, Montenero, A., Gnappi, G. and Lan, L., Crystallization behaviour in the system $MgO–Al_2O_3–SiO_2$. *J. Non-Cryst. Solids*, 1995, **192 & 193**, 529–533.